CH9900017

COLLOIDS IN THE MORTAR BACKFILL OF A CEMENTITIOUS REPOSITORY FOR RADIOACTIVE WASTE

E. Wieland, P. Spieler

Colloids are present in groundwater aquifers and water-permeable engineered barrier systems and may facilitate the migration of radionuclides. A careful evaluation of colloid concentrations is required to assess the potential effect of colloids on nuclide migration and, consequently, on the safety of a repository for radioactive waste. A highly permeable mortar is foreseen to be used as backfill for the engineered barrier of the Swiss repository for low- and intermediate-level waste (L/ILW). The backfill is considered to be a chemical environment with a potential for colloid generation and, due to its high porosity, for colloid mobility. In this contribution a novel in-house built particle counting device is described, and measurements of colloid concentrations in the pore water of backfill mortar are presented

1 INTRODUCTION

For the performance assessments of nuclear waste repositories, a detailed understanding of the transport mechanisms which govern the migration of radionuclides in the engineered barrier system and the surrounding geological formation is required. Colloids may facilitate radionuclide migration from a waste repository to the biosphere. Therefore, their impact is consequently addressed in performance assessments [1,2]. Three criteria must be met for inorganic colloids to facilitate the transport of radionuclides: (1) colloids must be present; (2) radionuclides must associate with the colloidal material; (3) colloids and the associated radionuclides must be transported through the aquifer. The first criterion is met: colloids are abundant in groundwater systems and have been found in groundwater samples collected from aquifers in different geological and hydrogeochemical settings [3]. However, their concentrations are usually too low to have an appreciable impact on nuclide transport. The second criterion is also met as colloidal phases appear to be effective carriers of strongly sorbing contaminants due to their relatively high surface area [4]. Note that radioactive waste contains strongly sorbing radionuclides such as lanthanides and actinides. Moreover, it has been shown that the migration of colloids and associated contaminants may occur in groundwater aquifers indicating that the last criterion may be fulfilled as well [3]. For the performance assessment of the planned Swiss repositories, a transport model has been developed accounting for colloid-facilitated radionuclide migration in the near and far fields [5,6,7]. Two important input parameters are required in the transport model: (1) The concentration of dispersed colloids for near- and far-field conditions and, (2) the distribution coefficient of a radionuclide between the colloidal and aqueous phase. Both parameters can be provided from laboratory and field studies. For example, an extensive investigation on colloids in crystalline rocks has been published [8,9,10], and field measurements at the Wellenberg site are still ongoing [11].

The objective of this contribution is to describe the use of a detection system which is employed at the Laboratory for Waste Management (LES) for measuring colloid concentrations at very low levels in liquid samples. A detailed description of the instrument will be given in the following section. Measurements of colloid concentrations in the pore water of highly permeable "Monokorn" mortar, known by Nagra designation as mortar M1, are then presented. The mortar material is currently favoured as backfill in the planned Swiss L/ILW repository. The backfill was specially designed to allow the release of gas which could be formed in the repository due to corrosion, and to ensure mechanical stability through the filling of voids between the waste containers. In the final section, the effect of the chemical composition of fluids on the colloid inventory is discussed.

2 COLLOID CONCENTRATION MEASUREMENT

In this context, the terms "colloids" and "particles" require a few explanatory comments. There is no unique view within the various scientific disciplines as to what colloids and particles actually are in size [12]. The situation is complicated by the fact that the definitions are mostly based on experimental techniques applied to discriminate colloidal and particulate materials. In this study, the main criteria for distinguishing colloids and particles is based on the presence of a chemical entity (organic or inorganic) which is generated or present in the system, is chemically stable, and small enough to be dispersed in suspension by Brownian motion. Hence, "particles" with diameters ranging from 1 nm to 1000 nm are denoted here as colloids. Larger particles with diameters >1000 nm may be efficiently retarded in the repository due to sedimentation or attachment to the bulk material of the near field rather than being dispersed in the pore water. The lower size limit is set to discriminate colloids from dissolved species (molecules and ions).

There is no unique method available which allows a complete analysis of colloids or particles, for example, the simultaneous determination of the concentration, size distribution and composition of colloidal or particulate material. Hence, information on the properties of colloids and particles is assembled from a combination of techniques. A particle counting system was recently put into operation at LES which allows us to detect colloids at low concentration levels and to evaluate the size distribution of colloid populations

over a broad size range. The counting device consists of commercially available sensors which operate *in-situ* on the principle of laser light scattering at single particles [13].

2.1 Description of the particle counting system

A schematic view of the particle counting system is given in Fig. 1. A high volume sampling flow of deionised water is generated in the water purification system to establish a flow rate of 500 mL min^{-1}. The samples are injected into the sampling flow using a HPLC pump at an injection rate of 200 to 2200 mL h^{-1}. The injection rate is dependent on the concentration range of the samples. Three sensors are employed in combination: a Horiba sensor (PLCA-311; Horiba Ltd., Kyoto, Japan) arranged in series with two PMS sensors (HVLIS-C200-Cor and HSLIS-M50; Particle Measuring Systems Ltd., Boulder, USA). After passing the sample cell of the PLCA-311 sensor, the sampling flow is split into two branches of different flow rates, 100 mL min^{-1} and 400 mL min^{-1}, as recommended for operation of the in-parallel arranged PMS sensors. Regulators control the sampling flow.

The sensors operate on the principle that light scattered by a liquid borne particle (or colloid) resident in a laser beam is directly proportional to its size. Particles of a given size scatter light through a given angle which increases with decreasing particle size. Therefore, colloids of the same size transiting the laser beam produce the same amplitude pulses and pulses of finite width. Since the samples are strongly diluted, detection of single particles is possible. The pulses of radiant energy are recorded by photodiode detectors which are oriented at 90° to the laser beam. A rectangular orientation greatly improves the signal-to-noise ratio. The pulses are amplified and their maximum amplitude stored with a conventional pulse height analyser (peak detection). Optical sensors are calibrated with standard size particles to establish the pulse vs. size interval curves.

Although operating on the same principle, the sensors differ with respect to the optical systems, data acquisition as well as the properties of the lasers and sample cells. The PLCA-311 counter operates with a Gaussian TEM_{∞} mode laser (10 mW, 480 nm). Despite the high resolution, it only incorporates three size channels with size thresholds ≥ 100 nm, ≥ 200 nm and ≥ 500 nm at standard sensitivity. Output data represent colloid concentrations above the threshold settings. The PMS sensors operate with a Gaussian TEM_{∞} mode laser (30 mW, 780 nm). The HSLIS-M50 is a 0.05µm threshold monitor unit incorporating 4 size channels. The sensor is connected to a PDS-PB data system. This instrument has been designed for fast and continuous real-time detection of colloids. The HVLIS-C200-Cor operates in the spectrometer mode incorporating a total of 8 size channels in the size range 200 nm to 5000 nm. The sensor is controlled by a MicroLPS data system. This instrument has been designed for applications where high flow rates are appropriate.

The particle counting system is controlled by an in-house developed PC compatible software based on DELPHI (Borland). The programme also allows data acquisition and data compilation. For data analysis and data treatment, however, commercially available programmes are employed.

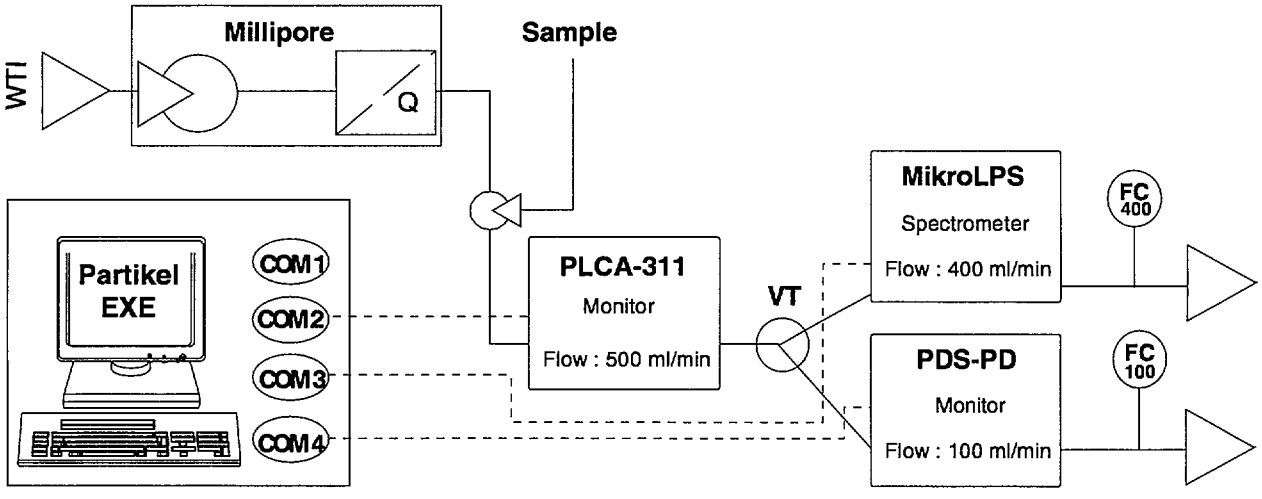

Fig. 1: Schematic representation of the particle counting system. The system consists of the following components: Millipore Milli-Q Plus water purification system (**Millipore**); HPLC pump for sample injection (**Sample**); a combination of three particle counters: Horiba PLCA-311 counter (**PLCA-311**), PMS HSLIS-M50/PDS-PB monitor (**PDS-PB**) and PMS HVLIS-C200-Cor/MicroLPS spectrometer (**MikroLPS**); flow splitting unit (**VT**); flow regulators (**FC**); PC for instrument control and data acquisition.

2.2 Specification of the particle counting system

The particle counting system was designed for measuring colloid concentrations and size distributions of natural samples. The specifications of the counter (PLCA-311), monitor (HSLIS-M50) and spectrometer (HVLIS-C200-Cor) differ with respect to sensitivity (smallest detectable colloid size), resolution (number of channels) and sampling rates (flow). Spectrometers operate with high resolution and relatively low sensitivity. Monitors are a new class of instrument with a high sensitivity, high sampling rates but relatively poor resolution. Optical counters have higher intrinsic resolutions, however, incorporating only a very limited number of size channels. A combination of sensors enables us to determine particle size distributions over the size range 50 nm to 5000 nm with a relatively high resolution (maximum 13 size channels) and at a very low concentration level (10^8 to 10^{11} particles L^{-1}). Note that the lower concentration limit is due only to particulate impurities present in Milli-Q water (Fig. 2).

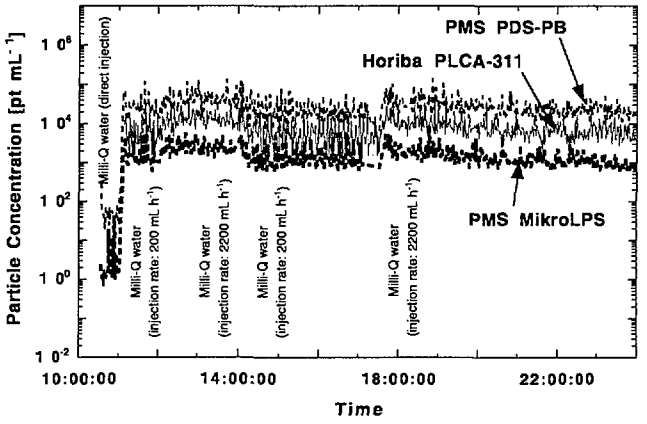

Fig. 2: Determination of the background of Milli-Q water. The colloid concentrations determined by the sensors are shown as a function of time. Purified water (Milli-Q water) was injected either directly into the sampling flow or added via injection pump (pump rates: 200 mL h^{-1} and 2200 mL h^{-1}, respectively).

2.3 Presentation of particle size distribution

A size spectrum with continuously decreasing particle concentrations at increasing particle size can be displayed in terms of a power-law distribution. It has been applied to display size distributions of atmospheric and stratospheric aerosol particles (micron and submicron size range) as well as sedimentary particles and suspended matter in the ocean (submillimeter size range) [14]. Numerous examples have demonstrated its wide applicability for representing size spectra of particles (or colloids) in natural systems. The continuous size distribution is defined by [15]:

$$\frac{dN(\varnothing)}{d\varnothing} = n(\varnothing) \qquad [m^{-3}\ m^{-1}] \qquad (1)$$

where $\varnothing$ is the linear dimension of the particles and $N(\varnothing)$ the concentration of particles of a given size (particles m^{-3}). For a graphical presentation of the analytical data, the continuous size distribution is approximated by a discrete differential size distribution with $dN(\varnothing)/d\varnothing$ given by the concentration of particles per unit of size $\Delta N(\varnothing_p)/\Delta\varnothing_p$. Here $\Delta\ \varnothing_p$ corresponds to the size interval ($= \varnothing_{p+1} - \varnothing_p$), and $\Delta N(\varnothing_p)$ denotes the cumulative concentration of particles in the size range $\varnothing_p$ to $\varnothing_{p+1}$ (bar height of the histogram). Since concentration and size can vary over several orders of magnitude, a log-log presentation is used to display particle concentration as a function of linear particle dimension:

$$\log\frac{\Delta N(\varnothing_p)}{\Delta\varnothing_p} = \log A - b\log\varnothing \qquad (2)$$

When laser scattering size analysis is applied for sorting particles into size fractions, the characteristic dimension $\varnothing$ represents the equivalent spherical-cross-section area diameter. A and b are empirical parameters of the particle size distribution. Particle populations of natural samples show size distributions with a slope -b typically ranging from about -1.8 to -4.5 [14].

2.4 Size distributions of model systems

To evaluate the performance of the particle counting system, test measurements on model systems were carried out. In these tests, particle suspensions with well-defined size distributions in the range 50 nm to 5000 nm were prepared from certified size standards (Polystyrene spheres). The slopes -b of the size distributions were approximately -3 and -4. In Fig. 3, measurements (symbols) and expected size distributions (lines) are displayed in accordance with the notation given in Eq. (2). The characteristic parameters logA and -b of the power-law distribution were calculated on the basis of known and measured particle concentrations. The tests show that the expected and measured parameters, i.e., intercept (logA) and slope (-b), agree well, indicating that the size distributions of particle suspensions which were prepared from size standards can be evaluated based on the measurements carried out with the particle counting system. For natural samples, however, some uncertainties remain due to the non-spherical shape and differences in the chemical composition of the particles. Hence, the following assumptions have to be made for natural samples: 1) natural particles scatter laser light in the same way as ideal spheres, 2) differences in the index of refraction of natural particles (e.g., quartz: $n_D = 1.544$ at 589 nm) and reference particles (e.g., polystyrene: $n_D = 1.59$ at 589 nm) are not large enough to cause any distortion of the size distribution. An interlaboratory comparison exercise in which different techniques were applied to enumerate colloid samples showed that these assumptions are well justified [8]. Measurements based on laser light scattering agreed with other sizing and counting techniques. One may thus infer that the single particle counting technique can provide rapid and accurate measurements of the particle concentrations and size distributions in natural samples.

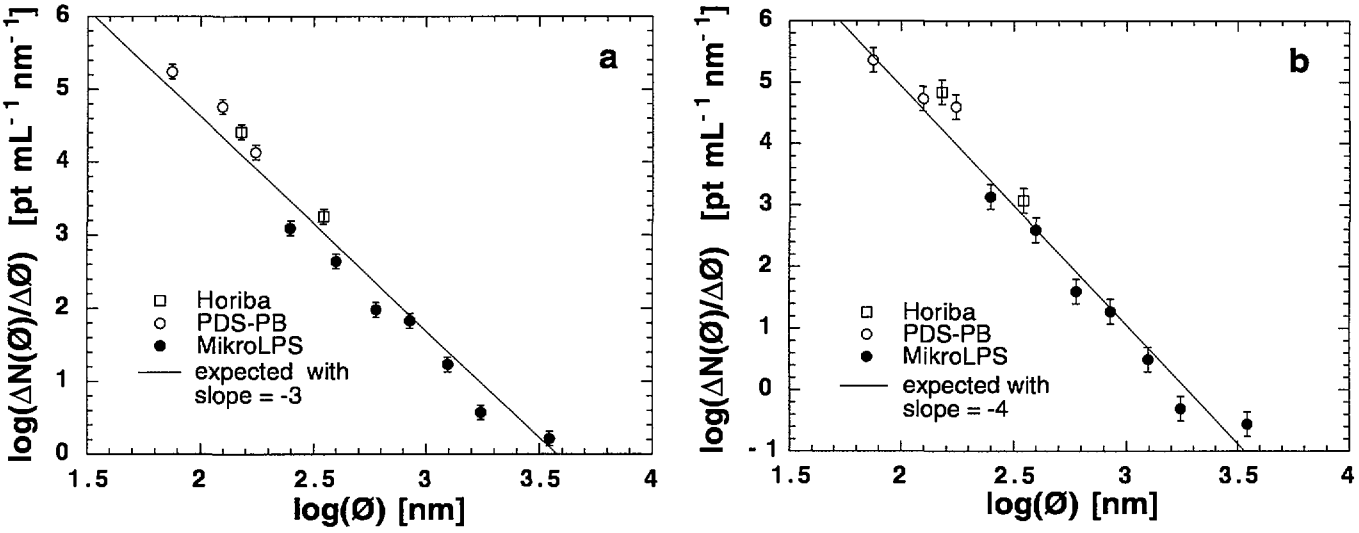

Fig. 3: Tests measurements with particle suspensions prepared from certified Nanosphere™ size standards. The model systems were prepared in such a manner to give particle size distributions with a) slope = -3 and b) slope = -4 (power-law distribution). Lines represent the expected decrease in the particle concentrations with increasing particle diameter (Ø). Circles indicate measurements of particle concentrations.

Table 1: Expected and determined values of the characteristic parameters (logA, -b) for two model systems. "Expected" values were calculated based on known particle concentrations in suspension. "Determined" values were evaluated from measured particle concentrations.

Slope -b expected	Slope -b determined	logA expected	logA determined	Corr. coeff. r
- (3.00 ± 0.03)	- (3.25 ± 0.21)	10.93 ± 0.09	11.44 ± 0.55	0.99/0.98
- (3.99 ± 0.07)	- (3.99 ± 0.23)	13.24 ± 0.19	13.09 ± 0.62	0.99/0.98

3 COLLOIDS IN THE PORE WATER OF MORTAR BACKFIILL

Measurements of colloid concentrations in the pore water of backfill mortar were carried out in lab-scale batch systems [16] and within the frame of the COLEX project. COLEX (COLumn EXperiment) was a large scale flow experiment with the goal of studying coupled gas and water transport processes in the backfill mortar M1 [17]. The study was carried out at the Institute for Building Materials (ETH Zürich) within the frame of the Swiss radioactive waste disposal programme. In the following, we concentrate on the COLEX experiments.

A schematic view of the experimental set-up is given in Fig. 4. The column was made of two elements each of which were filled with mortar M1 (total length = 2.7 m, diameter = 0.274 m). A constant flow of 30 mL min^{-1} of pre-conditioned water was maintained during operation using a peristaltic pump. The inlet was connected at the bottom of the column inducing a bottom-up water flow. Pre-conditioned water was prepared by mixing drinking water with Portland cement (water/cement ratio = 20). Injection cement water which was prepared in this manner was analysed for the major cement-derived elements, i.e., Ca, Na and K. The concentrations of Ca, Na and K were determined to be ~20 mM, ~3 mM and ~8 mM, respectively, indicating that the Ca concentration of the cement water was controlled by portlandite solubility which fixes the pH at ~ 12.5 (state II of the cement degradation) [18]. The colloid concentration of the cement pore water was found to be in the range of a few ppb. Samples were collected through the bottom and the top valves of the column (Fig. 4). Fig. 5 shows the colloid size distributions measured for a first series of pore water samples. The characteristic parameters of the size distributions are given in Table 2.

The colloid mass concentration was calculated on the basis of the power-law distribution. Assumptions have to be made concerning the shape and density of the colloidal material in order to express colloid number concentrations in terms of colloid mass concentrations. The volume distribution function can be written as:

$$\frac{dV}{d\varnothing} = \frac{\pi}{6}\varnothing^3 \frac{dN}{d\varnothing} \qquad (3)$$

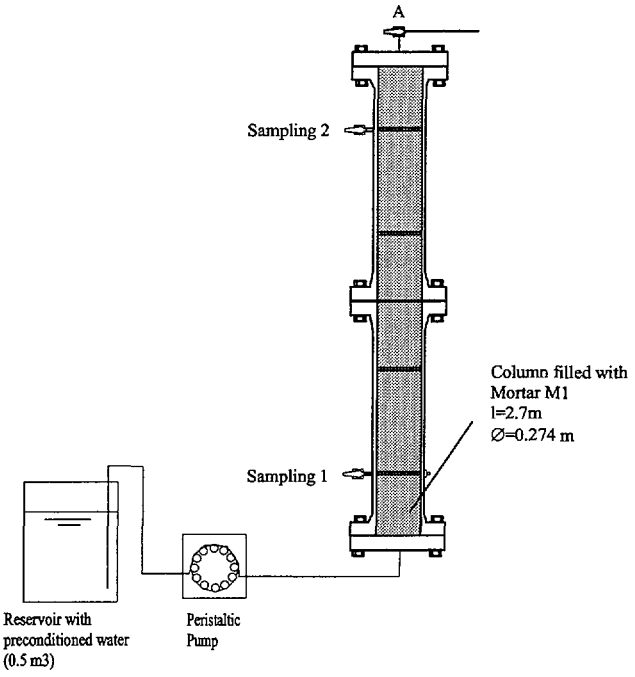

Fig. 4: Schematic view of the experimental set-up for the COLEX project [17].

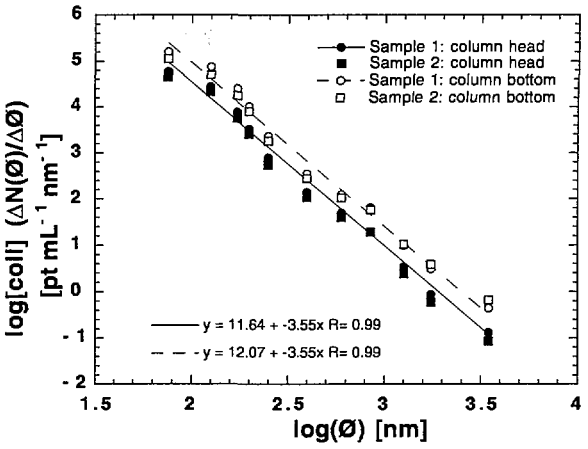

Fig. 5: Colloid size distributions in pore water of mortar backfill. The colloid concentrations of distinct size classes ($\Delta N(\varnothing)/\Delta\varnothing$) are shown as a function of the particle size ($\varnothing$) (range 50 nm to 5000 nm).

The mass distribution in the power-law approximation is then given by:

$$\frac{dm}{d\varnothing} = \rho \frac{\pi}{6} \varnothing^3 \frac{dN}{d\varnothing} \qquad (4)$$

with ρ as the density of the cement-derived colloids (ρ = 2000 g dm^{-3}). The mass concentration of colloids for a given size interval can be calculated by entering the function of the colloid number distribution as given in Eq. (2) into Eq. (4) and integrating the equation within the size limits $\varnothing_1$ (= 1 nm) and $\varnothing_2$ (= 1000 nm). Table 2 shows that the mean colloid concentrations of the samples were 15 to 60 µg L^{-1}. The uncertainties in the colloid mass concentrations are due to uncertainties in both logA and slope -b. An additional series of samples were measured at the end of the tracer migration study. The colloid mass concentrations of those samples were found to lie within the uncertainty ranges given in Table 2.

The pore water samples were also analysed for major cement-derived elements (Table 3). The Ca concentration was determined to be (23±3) mM indicating control by portlandite solubility. The results reveal that the chemical composition of the backfill pore water is in accordance with a cement pore water in state II of the cement degradation (pH ~ 12.5). Therefore, the colloid concentrations given in Table 2 can be taken as being representative of a degraded cement system.

Table 2: Characteristic parameters (logA, and b) of the power-law distribution as given by Eq. (2) and colloid mass concentrations using Eq. (4). The uncertainty factor results from the asymmetric shape of the power-law distribution.

Sampling	logA	Slope -b	Colloid Mass [µg L^{-1}] (size range 1 to 1000 nm)	
			Median	Uncertainty factor
Column head:				
Sample 1	11.64 ± 0.43	-(3.55 ± 0.16)	22	4.4
Sample 2	11.67 ± 0.32	-(3.62 ± 0.12)	16	3.2
Column bottom:				
Sample 1	12.07 ± 0.34	-(3.55 ± 0.13)	58	2.9
Sample 2	11.49 ± 0.34	-(3.35 ± 0.13)	45	3.0

Table 3: Chemical analysis of the pore water of mortar backfill

Element	Concentration [M]
Na	$(6.1\pm0.8)\times10^{-3}$
K	$(1.7\pm0.2)\times10^{-2}$
Ca	$(2.3\pm0.3)\times10^{-2}$
S	$(5.1\pm0.3)\times10^{-3}$
Si	$(6.6\pm0.9)\times10^{-6}$
Al	$(2.0\pm0.4)\times10^{-6}$
Mg	$(1.0\pm0.5)\times10^{-5}$

4 CHEMICAL COMPOSITION OF PORE WATER AND COLLOID CONCENTRATIONS

From theoretical and experimental studies it was shown that pore water velocity and the chemical composition of pore water (ionic strength and Ca concentration) may exhibit an influence on colloid mobility and concentration [10,19,20,21]. The water velocity affects the physical parameters which control colloid removal, e.g., transport to the collector surface. The water composition, on the other hand, affects the collision efficiency, that is sticking to the collector surface. It has been demonstrated that the dependence of the colloid deposition rate on the water velocity is weak at low to moderate flow velocities [20,21]. Increasing the water flow from 1 cm h^{-1} to 100 cm h^{-1} enhances the deposition rate of colloids by only a factor of 5 in columns filled with porous natural media, e.g., sandy soil and aquifer material. Moreover, a theoretical analysis of colloid mobility indicates that, at low to moderate flow velocities, the deposition rate increases with flow velocity by a power of zero to one third [21]. Therefore, the main factor governing colloid deposition in natural porous media and, consequently, the concentration of dispersed colloids is the chemical composition of the pore water.

In Fig. 6, colloid concentrations determined for cementitious systems are compared with measurements of the colloid concentrations in granitic groundwater samples [9]. The colloid concentrations of the water samples depend on the salt concentrations (ionic strength) rather than pH. Fig. 6b shows a trend to lower colloid concentrations with increasing ionic strength. In the cementitious systems the colloid concentrations were found to be lower than about 0.2 ppm. In state I of the degradation of a cementitious near field the ionic strength of the cement pore water was predicted to be around 0.3 eq L^{-1} ([Ca] ~ 2 mM) [18,22]. Consistently low colloid concentrations were observed when mortar M1 was in contact with a highly alkaline solution in batch systems (I ~ 0.3 eq L^{-1}) [16]. For state II of the cement degradation the ionic strength was predicted to be lower (~ 0.07 eq L^{-1}), but the Ca concentration is enhanced due to an increase in the solubility of portlandite at pH 12.5 ([Ca] ~ 20 mM) [18,22]. Low colloid concentrations are expected for such conditions, and this was confirmed in the COLEX study.

Studies on colloid mobility and colloid stability in natural porous media indicate that ionic strength and the Ca concentration are the chemical factors controlling colloid concentrations in laboratory as well as natural systems [10,20]. Laboratory studies on columns filled

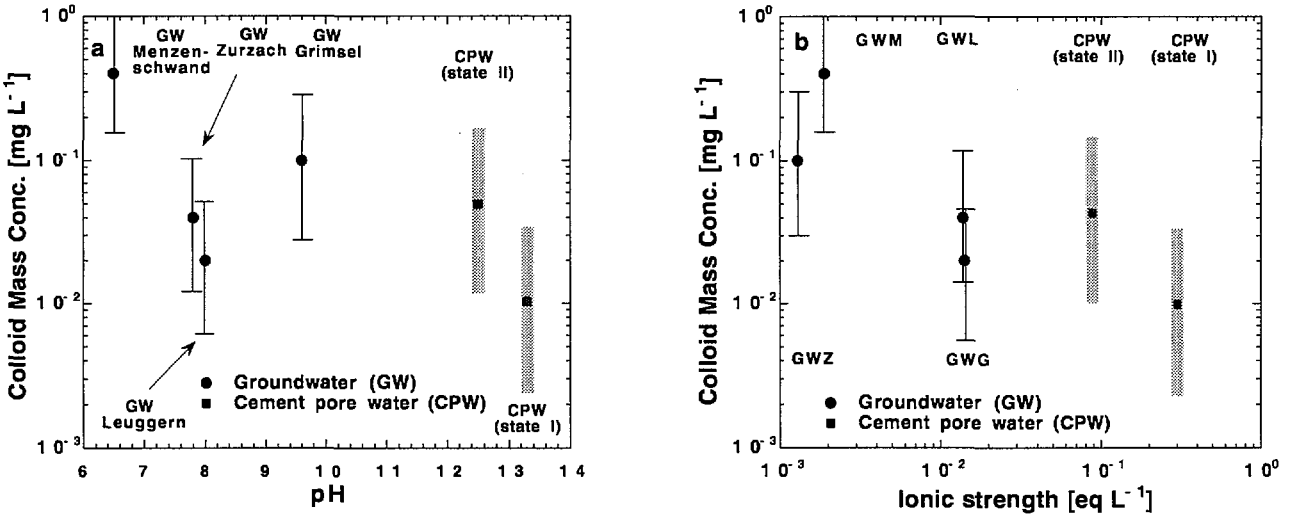

Fig. 6: Colloid mass concentrations of groundwater and cement pore water samples are shown as a function of pH and the ionic strength of the fluids. The values given for deep granitic systems with quasi-stagnant groundwater aquifers (GW) were taken from the literature [9]. Sampling sites were located in the alpine and prealpine area. Cement pore water (CPW) "state I" data were obtained by contacting backfill mortar M1 with a highly alkaline solution of ionic strength 0.3 M in batch systems [16]. CPW "state II" data are given in Table 2. Uncertainties in the data are estimated based on the ranges reported in Table 2.

with aquifer or soil materials show that a five-fold increase in ionic strength may enhance the colloid deposition rate and the collision efficiency α of carboxyl latex colloids [20]. In the experiments the sticking factor α changed from 0.1 to 1 (maximum value) based on an increase in the electrolyte concentration (NaCl) from 0.03 M to 0.11 M [20]. The influence of Ca on colloid stability was even more pronounced: an increase in the Ca concentration from 10^{-4} M to 10^{-3} M was reported to cause an enhancement of the collision efficiency by two orders of magnitude, i.e., from 0.01 to 1 [10,20]. Hence favourable chemical conditions for colloid removal by natural porous media are achieved at ionic strength > 0.1 M or Ca concentrations > 10^{-3} M, respectively. Under these conditions every collision of a colloid with the porous media results in attachment ($\alpha = 1$), and the deposition rate is limited only by the frequency of colloid-matrix collisions. Hence, one may conclude that the chemical conditions prevailing in the near-field environment of a repository are favourable for colloid-matrix interactions, giving rise to low concentrations of dispersed colloids and, therefore, a minor impact of colloids on radionuclide migration.

5 SUMMARY AND CONCLUSIONS

A particle counting system for the determination of particle concentrations at low levels and particle size distributions is described. The counting system operates on the principle of laser light scattering by single particles. A combination of sensors is used which allows measurements of particle distributions in the size range 50 nm to 5000 nm to be conducted. Tests on model suspensions which were prepared from certified polystyrene standard particles show that size distributions can accurately be presented on the basis of the measurements.

Colloid concentrations and size distributions were determined in cement pore water samples which were collected from a column filled with backfill mortar M1. The colloid mass concentration was estimated to be lower than about 0.2 ppm. Analysis of the pore water composition indicates that the backfill mortar had reached state II of the cement degradation.

The results of the colloid concentration measurements are in accordance with the hypothesis that the concentration of dispersed colloids in cement pore water is low due to the specific chemical conditions. That is, high ionic strength and Ca concentrations in the millimolar range prevail, which are favourable for colloid sorption on a collector surface or colloid removal due to aggregation. The low colloid concentrations are expected to have a minor impact on radionuclide migration.

6 ACKNOWLEDGMENT

We wish to thank D. Werner for his support during the installation of the particle counter, G. Mayer for assisting in pore water sampling and a plot of the Colex column, and J. Hadermann and M. Bradbury for helpful comments. Partial financial support by the National Cooperation for the Disposal of Radioactive Waste (Nagra) is gratefully acknowledged.

7 REFERENCES

[1] Nagra, "*Kristallin-1; Safety Assessment Report*", Nagra NTB 93-22, Wettingen (1994).

[2] Nagra, "*Endlager für schwach- und mittelaktive Abfälle (Endlager SMA); Bericht zur Langzeitsicherheit des Endlagers SMA am Standort Wellenberg, NW*", Nagra NTB 94-06, Wettingen, (1994).

[3] J.F. McCarthy, C.A. Degueldre, "*Sampling and Characterization of Colloids and Particles in Groundwater for Studying their Role in Contaminant Transport*", In: Environmental Particles Vol 2, J. Buffle & H.P. van Leeuwen (eds.), Lewis Publishers, Boca Raton, (1993).

[4] R. Grauer, "*Zur Chemie von Kolloiden: Verfügbare Sorptionsmodelle und zur Frage der Kolloidhaftung*", PSI-Bericht 90-65, Paul Scherrer Institut, Villigen, Switzerland, (1990).

[5] P.A. Smith, "*A Model for Colloid-Facilitated - Radionuclide Transport through Fractured Media*", PSI-Bericht 93-04, Paul Scherrer Institut, Villigen, Switzerland, and Nagra NTB 93-32, Wettingen, (1993).

[6] P.A. Smith, C.A. Degueldre, "*Colloid Facilitated Transport of Radionuclides through Fractured Media*", J. Cont. Hydrol. 13 143 - 146 (1993).

[7] P. Gribi, "*SMA/WLB: Einfluss von Nahfeldkolloiden auf den Nuklidtransport*", Nagra internal report, Wettingen, Switzerland, (1995).

[8] C.A. Degueldre, "*Colloid Properties in Groundwaters from Crystalline Formations*", PSI-Bericht 94-21, Paul Scherrer Institut, Villigen, Switzerland, and Nagra NTB 92-05, Wettingen, (1994).

[9] C.A. Degueldre, H.-R. Pfeiffer, W. Alexander, B. Wernli, R. Bruetsch, "*Colloid Properties in Granitic Groundwater Systems. I: Sampling and Characterisation*", Appl. Geochemistry **11** 677 - 695 (1996).

[10] C.A. Degueldre, R. Grauer, A. Laube, "*Colloid Properties in Granitic Groundwater Systems. II: Stability and Transport Study*", Appl. Geochemistry **11** 697 - 710 (1996).

[11] C.A. Degueldre, A. Laube, R. Keil, A. Scholtis "*A Study of Colloids at the Wellenberg Site; Status Report*", Nagra internal report (1998).

[12] J. Buffle, H.P. van Leuwen, "*Environmental Particles, Vol 1*", Lewis Publishers, Boca Raton, (1993).

[13] E. Wieland, P. Spieler, D. Werner, "*Aufbau und Inbetriebnahme eines Partikelzählsystems zur Bestimmung von Partikel- und Kolloidkonzentrationen in Flüssigkeiten*", Internal Technical Report TM-44-98-11, Paul Scherrer Institut, Villigen, Switzerland, (1998).

[14] A. Lerman, "*Geochemical Processes. Water and Sediment Environment*", J. Wiley & Sons, New York, (1979).

[15] S.K. Friedlander, "*Smoke, Dust and Haze*", J. Wiley & Sons, New York, (1977).

[16] E. Wieland, "*Colloid Concentrations in Cementitious Backfill: Monokorn Mortar and Quartz in Contact with Hyperalkaline Cement Pore Water*", Internal Technical Report TM 44-97-01, Paul Scherrer Institut, Villigen, Switzerland, (1997).

[17] G. Mayer, H.A. Moetsch, F.H. Wittmann, "*Large Scale Experiment for Water and Gas Transport in Cementitious Backfill Materials (phase 1) COLEX I*", NTB 98-03, Nagra, Wettingen, Switzerland, (in preparation).

[18] U.R. Berner, "*Evolution of Pore Water Chemistry during Degradation of Cement in a Radioactive Waste Repository Environment*", Waste Management **12** 201 - 219 (1992).

[19] M. Elimelech, J. Gregory, X. Jia, R. Williams "*Particle Deposition and Aggregation*", Butterworth-Heinemann, Oxford, (1995).

[20] R. Kretschmar, K. Barmettler, D. Grolimund, Y. Yan, M. Borkovec, H. Sticher, "*Experimental Determination of Colloid Deposition Rates and Collision Efficiencies in Natural Porous Media*", Water Resour. Res. **33** 1129 - 1137 (1997).

[21] L. Song, M. Elimelech, "*Calculation of Particle Deposition Rate under Unfavorable Particle-Surface Interactions*", J. Chem. Soc. Faraday Trans. **89** 3443 - 3452 (1993).

[22] F.B. Neal, "*Modelling of the Near-field Chemistry of the SMA Repository at the Wellenberg Site*", PSI-Bericht 94-18, Paul Scherrer Institut, Villigen, Switzerland, and Nagra NTB 94-03, Wettingen, (1994).